International Journal of Technology and Applied Science (IJTAS)

E-ISSN: 2230-9004 ● Website: www.ijtas.com ● Email: editor@ijtas.com

Rapikit: A Portable and Ecofriendly Sachet based Waste to Wealth Approach for Dual Removal of Arsenic and Nitrate Using Magnetic Biochar- Chitosan Composite: Isotherm Modelling, Characterization and Reusability Studies

Rahul Khatkar[1], Ramesh Kumar[2], Suman Nagpal[3]

[1,3]Department of Environmental Science, Indira Gandhi University, Meerpur (Rewari), Haryana, India.
[2]Department of Biotechnology, Indira Gandhi University, Meerpur (Rewari), Haryana, India.

Abstract:

Continuous exposure to Arsenic or Nitrate above safe value of (10 ppb of Arsenic, 45 ppm for Nitrate) leads to several health risks. Therefore, there is a need to develop cost effective reusable easy-to-use techniques for simultaneous removal of both contaminants. In the present work, waste to wealth development of a Rapikit, a novel, ready-to-use Pouch (2.76 inch * 1.97 inch) using empty teabag sachets filled with composite of magnetic biochar and chitosan was developed. The prepared composite was characterized by using Raman spectroscopy, FTIR, SEM, and XRD techniques. The results showed high porosity and presence of functional groups that are responsible for efficient removal of pollutants. In the batch adsorption experiment, The composites, in the optimized conditions i.e. pH 10 with a 1.5 g/L dose within 60 minutes of contact time at 25°C showed 97 % of arsenic removal efficiency as well as, and 90% removal efficiency for Nitrate at its optimized pH 7 with a 2.0 g/L dose and 80 minutes of contact time. The isotherm studies revealed that Arsenic adsorption followed the Langmuir isotherm with a maximum adsorption capacity of 21.37 mg/g and a Separation Factor value of 0.0607, indicating favorable adsorption for Arsenic. But in case of Nitrate adsorption, the composite fit the Freundlich isotherm (R^2 = 0.98), reflecting surface heterogeneity, with a maximum adsorption capacity of 2.43 mg/g for Nitrate. Importantly, when Rapikit used concurrently in mixed spiked water solutions at pH 6.9, the positive synergy of the composite enhanced the adsorption kinetics, resulting in a 97.67% Arsenic removal and 90.00% Nitrate removal within just 30 minutes of contact time. It showed negligible reduction in removal efficacy up to five regeneration cycles. This positive synergy of composite adds the advantages of chitosan for enhanced adsorption capacity and magnetic properties of biochar that facilitate the strong chemical interaction with the contaminants. Hence, Rapikit which showed the waste-to-wealth approach by transforming waste wood biomass into a value-added adsorbent and has great potential for scalability, provides a portable, eco-friendly, and user-friendly kit for the dual removal of nitrate and arsenic.

Keywords: User friendly, Rapikit, Magnetic Biochar-chitosan composite, Arsenic, Nitrate, Langmuir isotherm

1. Introduction

Water pollution remains a disastrous situation despite industry resolutions for the benefit of people worldwide [1]. Heavy metals [2], inorganic solutes (Kumar et al., 2023), and organic pollutants [4] due to industrial leaching or effluent discharge [5] may be caused contamination. Out of them, Arsenic and Nitrate contamination is the leading issue in front of environmental concerns or public health concerns, leading to Arsenicosis, skin lesions, cardiovascular disease, or carcinogenesis in humans [6]. Although Nitrate does not cause health issues, its toxicity, such as methemoglobinemia in young infants, was due to the reduction of Nitrate into nitrite, which reduced the binding efficiency of hemoglobin for oxygen [7]. In chronic intake, Nitrate causes gastrointestinal disorders and endocrine disruption [8].

Arsenic and Nitrate contamination become an alarming issue, particularly in agricultural regions, because Arsenic, being of geological origin, can leach into groundwater through natural processes as well as human activities such as mining and irrigation with polluted water, while excessive fertilizer use, increase the Nitrate levels in groundwater, resulting in the water of death [9]. Around 300 million people worldwide got affected by the poisoning of Arsenic [10], or 60 million of the population are associated with chronic health issues related to the consumption of groundwater contaminated with Nitrate [11]. Keeping in view the deadly effect, the World Health Organization (WHO) standardized the value of 10 ppb for Arsenic (World Health Organization, 2019) or 50 ppm for Nitrate in drinking water [12].

To meet the WHO standard, the contaminated water should be treated to remove Nitrate or Arsenic. In a way, various conventional techniques were used for the removal of Arsenic as well as Nitrate from the water, such as electrocoagulation [13], [14], chemical precipitation [15], ion exchange [16], [17], reverse osmosis [18], [19], [20], [21] and electro dialysis [22], [23], [24]. However, these traditional techniques have significant limitations, i.e., they are costly, less effective, generate high brine by-products, are hard to operate, and need expertise.

To overcome these adsorption-based technologies, which are based on chemical [25] or herbal-based adsorbents [26] for the decontamination of water considered as a convenient method because of simple to operate, minimum chemical use, highly flexible or economical with high efficiency [27]. Various adsorbent were used for the removal of Nitrate or Arsenic such as activated carbon [28], [29], clay adsorbents [30], [31], zeolites [32], [33], chitosan [34], [35], metal nanoparticles [36], [37], biochar [38], [39], activated alumina [29] and carbon nanotubes [40], [41]. Compared to typical adsorbents such as activated carbon or clay minerals, magnetic biochar and chitosan-based adsorbents have benefits that can lead to more effective, efficient, and environmentally friendly water treatment solutions. Combining magnetic characteristics with natural biopolymers can also result in synergies that improve the performance of both materials in water decontamination.

To the best of the knowledge, no user-friendly reusable adsorption composite has been explored that demonstrated dual removal effectiveness for Arsenic and Nitrate from water in the batch adsorption, as well as an easy-to-use kit. To validate the superior performance of the developed magnetic biochar–chitosan composite, its adsorption efficiency was compared with other adsorbents. The comparison highlights the improved dual removal efficiency of the present material toward both arsenic and nitrate.

The current study also demonstrates the development of a Novel, ready-to-use Rapikit (2.76 inch * 1.97 inch) , which demonstrates the dual removal efficiency for arsenic as well as nitrate. The Rapikit was filled

with waste-derived magnetic biochar and chitosan composite, which showed the waste-to-wealth approach by transforming waste wood biomass into a value-added adsorbent. The use of domestic wood waste for the composite preparation ensures a low-cost, eco-friendly water decontamination solution and fulfils the concept of SDG 6 (Clean water). This offers a portable, sustained, user-friendly Rapikit suitability for all types of users, i.e. rural households as well as common people.

2. Materials and method:

2.1. Chemical and reagents

All the chemicals, including ferric chloride ($FeCl_3$), ferrous sulfate ($FeSO_4$), sodium hydroxide (NaOH), hydrochloric acid (HCl), glutaraldehyde, acetic acid (CH_3COOH), chitosan flakes, ethanol, sodium Nitrate and sodium meta-arsenite were of analytical grade. They purchased from HI Media Pvt. Ltd. Empty tea bag sachet purchased from Amazon, manufactured by Lipetol. A stock solution of sodium Nitrate and Arsenic having a concentration of 100 ppm prepared by adding 0.137 g of sodium Nitrate and 0.173 g of sodium meta-arsenite in 100 ml of distilled water. All other solutions of Nitrate and Arsenic used in the study were prepared by the subsequent dilution from the stock solutions, and the experimental results were analyzed.

2.2. Preparation of Adsorbent

2.2.1. Collection of shipping waste wood

The waste wood collected from households is used as packaging material. The collected wood was cleaned and dried in the sunlight for three or four days, and after that, the wood was cut down into small pieces to prepare adsorbent.

2.2.2. Preparation of Magnetic biochar

The magnetic biochar was prepared using the liquid precipitation method, which was reported to have some modifications [42]. The wood pieces were transferred into the muffle furnace for the pyrolysis of the materials at specific conditions, such as temperature 300 °C for 60 minutes. The materials were crushed using a pestle and mortar and sieved for a uniform size. The black granular biochar was obtained and washed twice or three times using distilled water followed by ethanol until the filtrate was crystal clear without coloring properties. Afterwards, the biochar was dried in a hot air oven at 70 °C until all the moisture evaporated. 1 g of biochar was added to the 100 ml of distilled water and stirred for 10 minutes till hominization. After that, the mixture of ferric chloride and ferrous sulfate having proportion in ratio 10:3 was added into the suspension of biochar and stirred for 1 hour at 200 rpm using the magnetic stirrer at room temperature, which was followed by the addition of 1M NaOH solution dropwise into the suspension for adjusting the pH of the solution to 10. The prepared suspension was incubated for 24 hours at 25 °C. After the incubation, the black precipitate was filtered and washed several times with distilled water and ethanol to remove the coloring properly. Then, it was dried at 60 °C in a hot air oven for 2 hours to remove moisture.

2.2.3. Preparation of Magnetic biochar-chitosan composite

The protonated chitosan was prepared by adding 3g of chitosan flakes into 1 % acetic acid solution and stirring for 2 hours till hominization of the suspension. After that, 1 g of magnetic biochar (MB) was added into the chitosan suspension and stirred for 30 minutes using a magnetic stirrer, followed by adding 25 % glutaraldehyde (Glu) drop by drop into the suspension. After that, the suspension was left for 24 hours for chemical modification and crosslinking between the protonated chitosan and magnetic biochar. The next

day, a black gel composite formed after the incubation, which was dried at 60 °C for 6 hours using a hot air oven. After drying, the product was crushed using a pestle and mortar and sieved for a uniform size.

2.3. Fabrication of Rapikit for the removal

A sachet (2.76 inch * 1.97 inch) was taken and open the sachet carefully without tearing, followed by the weighing of the composite powder, i.e. 1.0 g and filled the sachet with the composite powder evenly but not packed tightly as this does not hinder the adsorption and close the lid of the sachet with the 1-2 pins of the staple to avoid the separation of powder while in use. Store the sachet in a cool, dry place away from the moisture area until it is used, as shown in Figure 1. The sachet was dipped into the solution of Nitrate or Arsenic for minutes, and after that, the sachet was taken out, and the solution was analyzed.

3. Characterization of Magnetic biochar-chitosan composite

3.1. Scanning electron microscope:

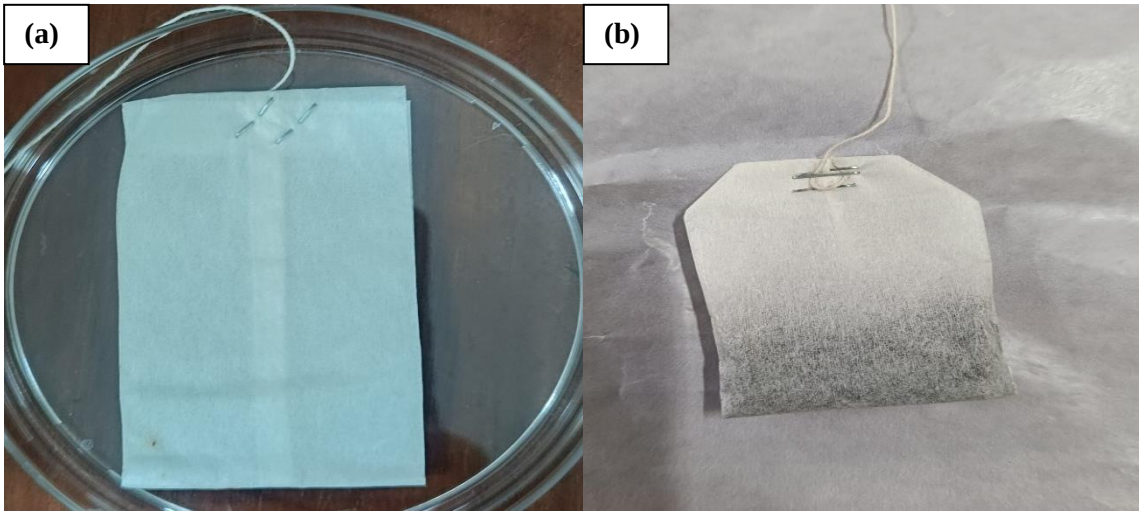

Figure 1 depicts (a) The Empty sachet kit **(**b) Rapikit filled with the waste wood derived magnetic biochar – chitosan composite

The scanning electron microscope (SEM) studies the sample's size and morphology (homogeneity or heterogeneity). It examined the sample topography by focusing the electron beam by spattering a thin layer of gold to prevent the sample's electrical charging and provide a homogeneous surface to promote secondary electron emission for imaging purposes and to analyze the porosity of the surface. The sample was characterized using a High-resolution field emission scanning electron microscope with EDS (FE-SEM) 7610F Plus/JEOL with a resolution of 0.8 nm@ 15Kv and 1.0 nm @1Kv.

3.2. Fourier transform infrared spectroscopy:

It is a technique for identifying the functional groups of the analyte that vibrate either by stretching or bending by interacting with the specific wavelength of light (infrared region). The sample was analysed using a Fourier transform infrared spectroscopy (FTIR) Perkin Elmer spectrum IR version 10.6.2 with a scan range of 4000-400 cm^{-1}.

3.3. X-ray diffraction :

The X-ray diffraction (XRD) technique examines a sample's crystalline properties. The sample was characterized using a multipurpose XRD system model—Smart lab 3kW, make—Rigaku, by applying voltage 40 eV, thin film XRD2, Range 1 to 157, And an angular scanning speed per minute of 2-10.

3.4. Raman microscopy:

Raman spectroscopy technique is used to characterize the materials based on the molecular vibration. The sample was characterized using the Renishaw Invia Raman microscope.

4. Application of the Magnetic biochar-chitosan composite for the removal of Arsenic and Nitrate

The prepared and characterized Magnetic biochar-chitosan composite was utilized to remove Arsenic and Nitrate in batch mode.

4.1. Batch adsorption study:

Batch adsorption studies were conducted to determine how modifying factors such as adsorbent dose, concentration, contact time, and solution pH affect the composite removal effectiveness for Nitrate and Arsenic removal. The batch experiment assay was conducted separately for the removal of Arsenic having a concentration of 15 ppb as well as Nitrate having a concentration of 10 ppm by taking an aqueous solution of 100 ml of solution in 250 ml of a conical flask that was stirred at 300 rpm followed by the filtration and the filtrate which was analyzed using the Aquasol Arsenic test kit for the Arsenic and Aquasol Nitrate testing kit or Nitrate standard curve at 202 nm using the Shimadzu UV-Visible spectrometer for the Nitrate.

4.2. Optimization of kinetic parameters:

The optimization of kinetic parameters was done to improve the removal efficiency of adsorbent for the Nitrate and Arsenic in the aqueous solution. The kinetic parameters, such as the effect of pH on the removal efficiency, were analyzed by measuring the adsorption of Nitrate and Arsenic by changing the pH value from 3.0 to 12 at regular intervals of 2 having a concentration of 15 ppb for Arsenic or 10 ppm for Nitrate, by keeping other parameters such as temperature, Incubation time and Adsorbent dose constant.. The pH of the aqueous solution was adjusted using 0.1M NaOH and 0.1M HCl, then measured with a Eu-Tech pH meter.

The effect of temperature on the removal efficiency of waste derived composite was evaluated by varying the temperature from 20°C - 40°C. The reading were taken at regular intervals of 5°C, where the concentration of 15 ppb for Arsenic or 10 ppm for Nitrate for constant pH, incubation time and adsorbent dose.

The effect of contact time analyzed after optimizing the pH condition for the removal by changing time intervals of 10 min to 120 min having a concentration of 15 ppb for Arsenic or 10 ppm for Nitrate and keeping other parameters such as temperature, pH and Adsorbent dose constant.

The effect of adsorbent dose on the removal efficiency of composite for Arsenic as well as nitrate was studied by varying the dose amount from 10 mg to 250 mg. The reading were taken with regular intervals of 50 mg for 100 ml of solution having a concentration of 15 ppb for Arsenic or 10 ppm for Nitrate by keeping other parameters such as pH, Incubation time and Temperature constant.

The effect of the concentration of analytes was analyzed after the finding of the optimized condition of the kinetic parameters (adsorbent dose, contact time, temperature and solution pH), and the maximum removal efficiency for the Arsenic and Nitrate calculated by estimating the percentage of adsorption by using the given formula:

Percentage of Removal (%) = $\{(C_o - C_{t/} C_o)\} \times 100$

C_o is the initial concentration of the analyte, and C_t is the final concentration of the analyte, which remained after the adsorption assay for the particular contact time.

The equilibrium sorption study for the removal of Arsenic and Nitrate was carried out by taking optimized kinetic parameters concerning different concentrations of analytes, i.e. 15 ppb to 100 ppb for Arsenic and 2 ppm to 20 ppm for Nitrate in 250 ml of conical flask stirred at 200 rpm on the magnetic stirrer. After that, the solution was filtered and analyzed, and the quantity of analytes adsorbed in the solution was determined by using the mass balance equation that Vanderborght and Van Griekenm reported.

Adsorption Capacity Q_o (mg/gm) = [(Co - Ce)] x V/m

Where Q= the amount of analytes adsorbed by the adsorbent from the solution, V= volume of the analyte solution that had taken, m= weight of adsorbate in grams, C_o is the initial concentration of the analyte, and *Ce* is the final concentration of the analyte that remained after the adsorption assay. After that, the data was used to compute the adsorption isotherm model and fitted with the Langmuir, Freundlich and Temkin isotherm model.

5. Result and discussion

5.1. Characterization of the waste derived Magnetic biochar-chitosan composite

5.1.1. Scanning electron microscope (SEM):

The SEM image of Magnetic biochar showed a rough, porous structure with the numerous of cavities and irregular texture of the surface as shown in Figure 2 (a) and crosslinking as shown in figure 2 (b) formed the Composite, it showed comparatively smoother surface because of the chitosan coating as in Figure 2 (c) it showed the partially covered of the porous structure by the chitosan layer which appeared as thin film or aggregated flakes on the surface of the composites. There morphological difference confirmed the successful modification of the composite surface.

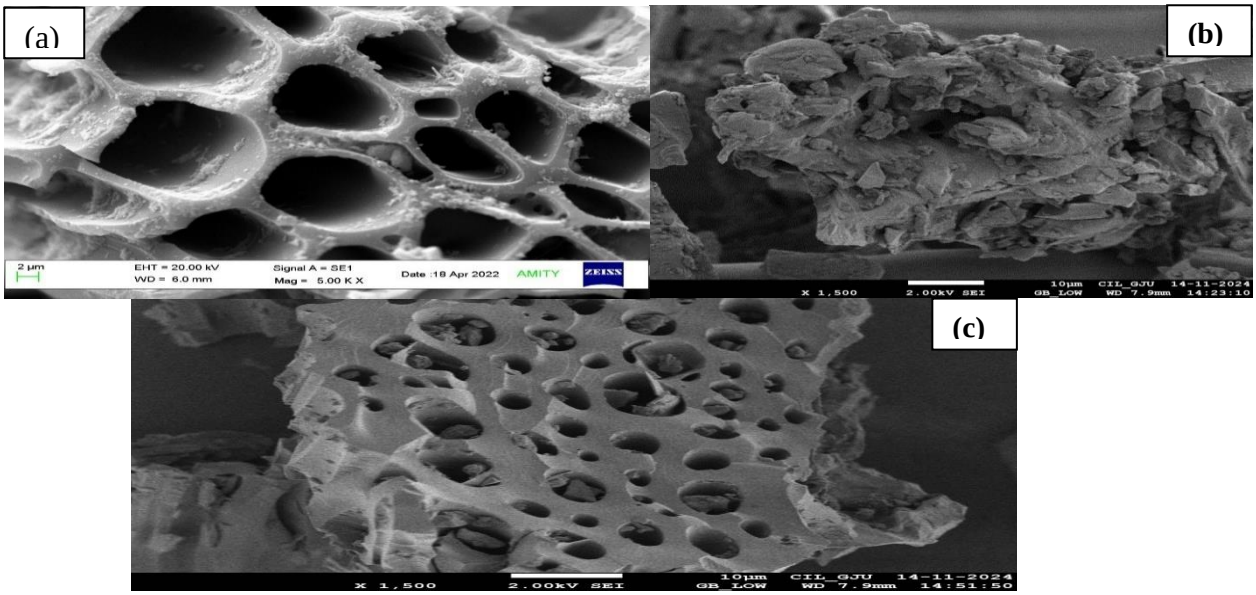

Figure 2. Scanning electron microscopy (SEM) images of the Magnetic biochar-chitosan composite (a) Magnetic biochar (b) the crosslinking or mesh like structure of the composite. (c) Chitosan – Magnetic biochar Composite

5.1.2. X-ray diffraction (XRD):

XRD was used to determine the crystallinity or amorphous nature of adsorbents. The results revealed a broad and small peak 2 θ between 20 and 90 °, indicating the amorphous nature of the adsorbent, and a large peak with high sharpness at 25 °, indicating some percentage of crystallinity with a crystallinity index of 0.3977 and a full width at half maximum (FWHM) of 0.5888 with a maximum grain size of 14.47 nm, implying chemical modification for the experimental study as shown in Figure 3.

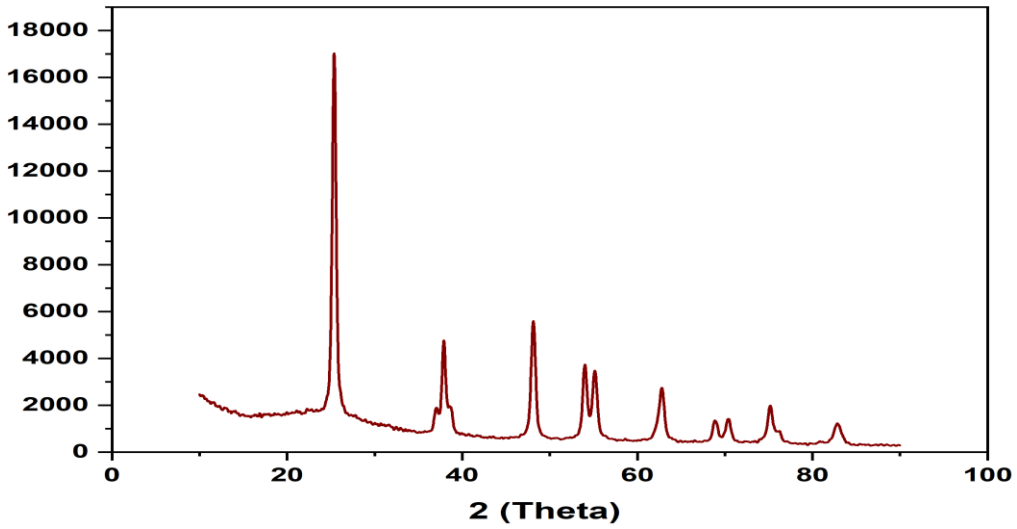

Figure 3. X-ray diffraction pattern of the Magnetic biochar- chitosan Composite

5.1.3. Fourier Transform Infrared spectroscopy (FTIR):

The functionalities relating to chemical bonds and surface functional groups were observed using Fourier Transform Infrared spectroscopy (FTIR) with a scan range of 4000-400 cm^{-1}, as shown in Figure 4. The emergence of a strong and broad peak at around 3443.57 cm^{-1} was attributed to the stretching vibration of the OH-functionalities of alcohol or the aldehyde class. The peak at 2920 cm^{-1} or 2854 cm^{-1} was due to the antisymmetric stretching vibration of C-H bonds [43]. A modest or wide peak at 1623 cm^{-1} was associated with the N-H bending vibration of the amine class, corresponding to the chemical alteration of the adsorbent with glutaraldehyde. When compared to magnetic biochar, an absorption peak at 1383 cm^{-1} was found to be Stronger and sharper, indicating chemical alteration with S=O bond stretching. Magnetic loading revealed an absorption peak at 625 cm^{-1} caused by stretching vibrations of the Fe-O groups, and similar result was reported by Azari et.al.2016 in the study of mercury extracting from aqueous solution by using the Iron oxide modified chitosan nanocomposites [44]. A small absorption signal at 1217 cm^{-1} suggested a C-N (amino) bond and efficient glutaraldehyde crosslinking of the adsorbent confirmed with the similar result reported by Li et.al. 2013 in synthesis and characterization and antibacterial activity of cross-linked chitosan by using the glutaraldehyde [45].

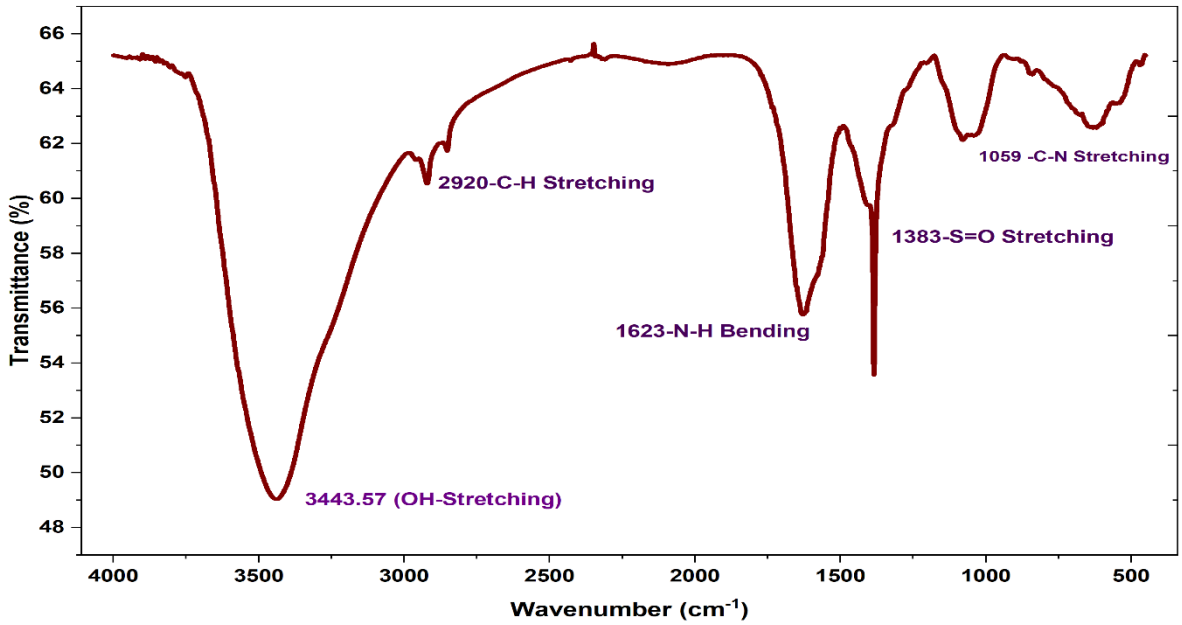

Figure 4. FTIR spectrum of the Magnetic biochar-chitosan composite

5.1.4. Raman spectroscopy:

The Raman spectroscopy method was used to analyze the degree of graphitization of carbon-based materials, as well as the degree of defects caused by changes in the materials' chemical lattice structure. Figure 5. Depicts the Raman spectra of the magnetic biochar chitosan composite adsorbent. The result showed the presence of the D band and G band at the specific value of 1386 and 1600 with blue shifting or the increment in the intensity of peaks, which manifestation marks for the linking between the protonated chitosan and magnetic biochar. The D band, named the disorder band, was generated by the

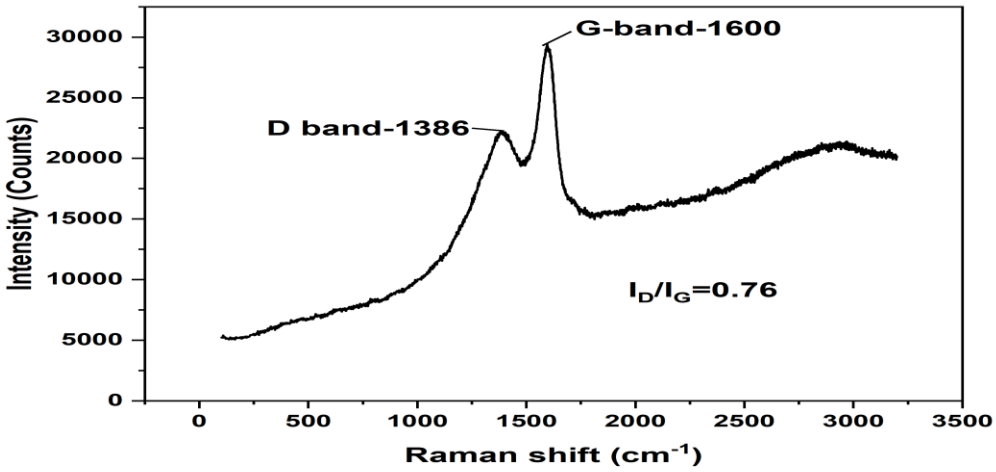

Figure 5. Raman Spectra of the Magnetic biochar-chitosan composite

breathing mode of the sp^2 carbon atom and initiation by defects in carbon structure that appeared as a high

value of disorder in the case of material that caused shifting from 1350 to 1386 in the case of adsorbent. The intensive value of ratio I_D/I_G observed as the extent of disorder and graphitization of materials, which appeared as 0.76 for the adsorbent, which resulted in the formation of composite adsorbent for the removal of Nitrate as similar results was reported by the Reis et al 2023 in study of nitrogen doped biochar for the removal of acidic dye [46].

5.2. Adsorption study and optimization of the kinetic parameters

The batch study was done by changing the concentration of Analytes i.e. Arsenic and Nitrate solution with the Standard method of analysis followed by the experiments that determined the optimized conditions including pH of solution, temperature, incubation time, Adsorbent dose and concentration of the solution to attain the maximum removal of the analyte from the solution.

5.2.1. Optimization of pH

The result showed that in the case of Arsenic the removal efficiency for the Arsenic from the aqueous medium was gradually increased with increasing the pH from 5.0 to 10.0 as shown in Figure 6 (a), and at 10.0, maximum removal efficiency for Arsenic was observed because of at pH 10 electrostatic interaction between the Arsenic ion and functionalities (Carboxyl group, amine group) in the surface of composite was enhanced, formed the stable complexes as compared and less interference from other ions [47]. So, further optimization experiments were done by keeping the pH 10 in case of Arsenic removal. In the case

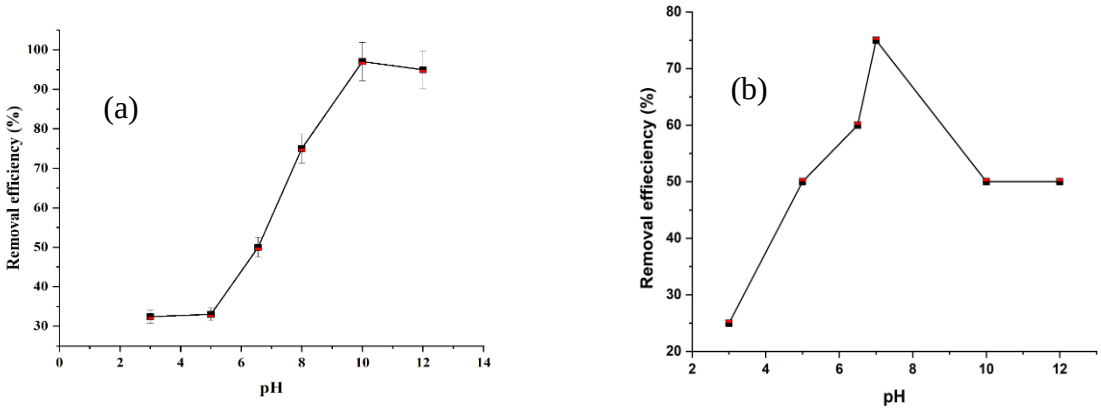

Figure 6 Effect of pH change on the removal efficiency (a) for Arsenic (b) for Nitrate

of Nitrate, the removal efficiency was increased from 3 to 7 and reached maximum removal at pH 7, as shown in the Figure 6(b). Further experiments for the optimization were done by keeping the optimized pH either for the Arsenic or the Nitrate removal.

5.2.2. Optimization of contact time

The result showed that the removal percentage increased as the contact time between the adsorbate and solution increased from 10 to 120 minutes by keeping the other kinetic parameters constant. The removal efficiency was reached at a maximum after the contact time of 60 minutes, as shown in Figure 7. That is why the result concluded that further experiment study done by keeping the pH 10 solution for 60 minutes of contact time in case of Arsenic removal. In the case of Nitrate, the percentage effectiveness of removal increased from 20% after 10 minutes of contact time to 90% after 80 minutes, as indicated in the figure 7 (b). After that point, the efficacy remains constant due to the saturation of available pore areas or the limited availability of active binding sites for electrostatic interaction with Adsorbate at that adsorbent dosage.

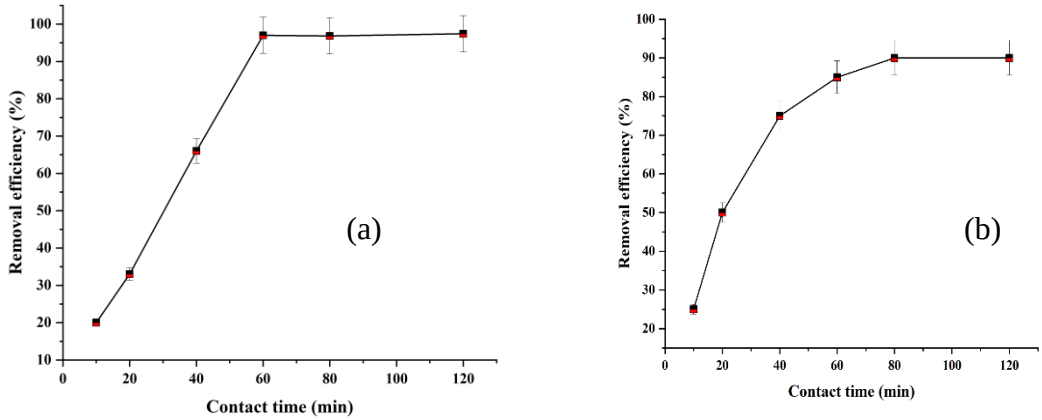

Figure 7 Effect of contact time on the removal efficiency (a) for Arsenic (b) for Nitrate

5.2.3. *Effect of Temperature*

The effect of temperature on the removal efficiency of Magnetic Biochar – chitosan composite (MBC-Composite) for Arsenic as well as Nitrate was studied at optimized contact time and pH with the regular intervals of 5°C. The result showed the increase in removal efficiency as the temperature increased and showed the maximum removal efficiency at 25°C because of enhanced mobility of Arsenic ions and increased interaction with the functional group present on the surface of MBC- Composite Above this temperature, the efficiency gradually decreased might due to weakening of bond interaction, desorption, alteration in surface integrity of the composite (Figure 8(a)). But in case of Nitrate the result showed the increase in removal efficiency as the temperature increased and showed the maximum removal efficiency at 25°C because of enhanced energy which promote the interaction between the Nitrate ion and active

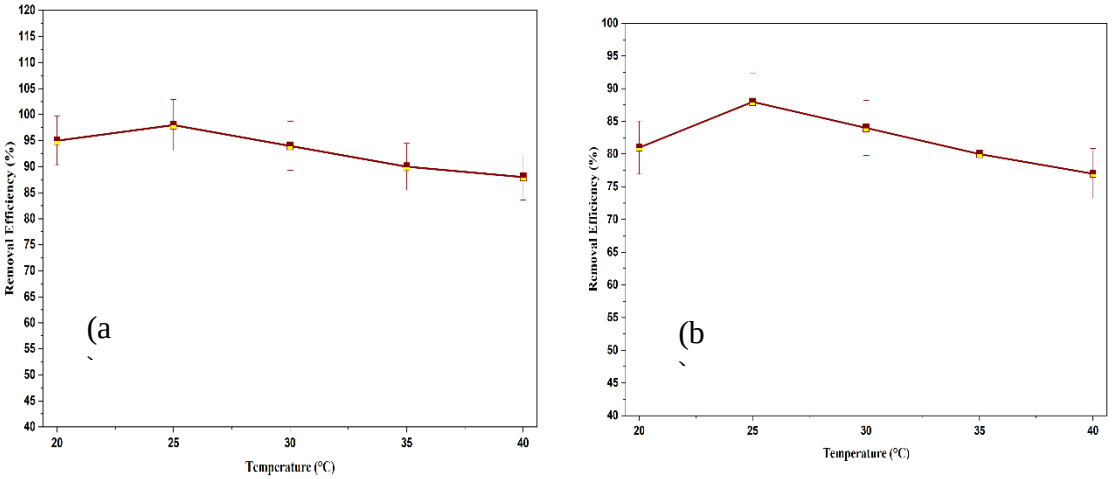

Figure 8 Effect of temperature on the removal efficiency (a) for Arsenic (b) for Nitrate

surface of MBC- Composite, and above this temperature, the efficiency gradually decreased because of high temperature might be attributed to the weakening of adsorption bond between the MBC- Composite surface and Nitrate and desorption of previously adsorbed Nitrate. The high temperature might cause the weakening of chitosan functional group or hydrogen bonding on the surface as shown in Figure 8 (b).

5.2.4. Optimization of adsorbent dose

The result revealed that the effectiveness of the material for the removal of Arsenic was rising as the dosage of the adsorbate increased from 10 mg to 250 mg for 100 ml of Arsenic solution having concertation of 15 ppb by maintaining other kinetic parameter in optimized conditions as depicted in figure 9 (a). The material's adsorbate dose of 1.5 g/l resulted in a maximum Arsenic removal effectiveness of 97 percent. In case of Nitrate removal, the result showed that increasing the adsorbent dose from 50 mg to 300mg /100 ml, which typically enhances Nitrate removal, as more active sites are available for Nitrate ion adsorption. However, the trends follow till the 200 mg/100 ml (2.0 g/L) showed the maximum removal percentage, beyond which the removal efficiency showed no significant change in value, as shown in Figure 9(b). Above certain adsorbent dosages, the available adsorption sites become saturated, resulting in a lower effective surface area per unit mass of adsorbent. Furthermore, high-dose adsorbent might cause agglomeration, restricting the adsorbent's interaction with the Nitrate ions.

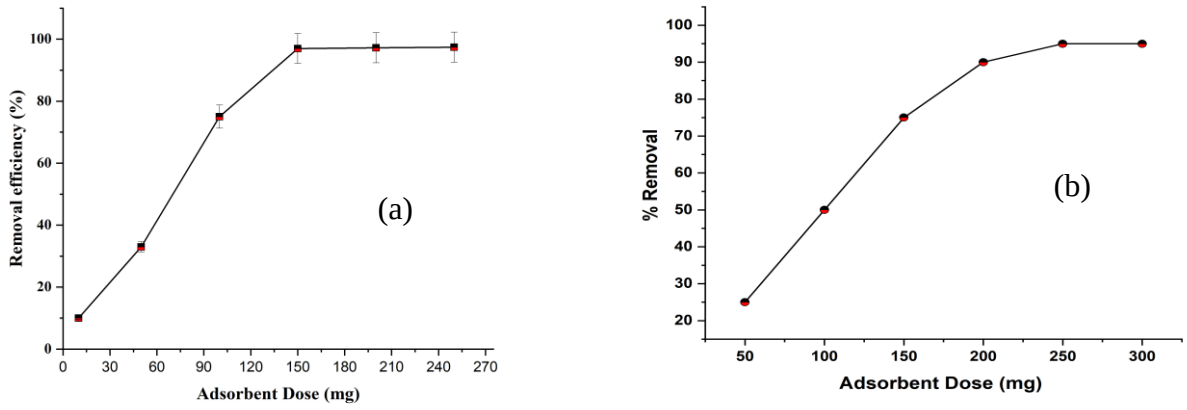

Figure 9 Effect of adsorbent dose on the removal efficiency (a) for Arsenic (b) for Nitrate

5.3. Adsorption isotherm study

The equilibrium sorption experiments for Arsenic or Nitrate were assessed by utilizing the optimal dosage of the adsorbate in 100 ml of various concentrations of solutions, which were filtered and the removal efficiency was examined. In the case of Arsenic, the percentage of removal was evaluated in a concentration ranging from 15 ppb to 100 ppb in the optimized condition of pH 10 for 60 minutes of contact time as shown in Table 1. The solution was filtered, and analyze the removal efficiency. But in the case of Nitrate as given in Table 2, the concentration ranged between 2 ppm to 20 ppm, and the data obtained were fitted for the following isotherm model, i.e. Langmuir isotherm, Freundlich isotherm and Temkin as presented.

5.3.1. Langmuir isotherm model

The Langmuir model demonstrated the monolayer adsorption phenomenon, indicating that only a limited number of sites on the adsorbent surface are accessible for adsorbate adsorption; thereafter, the adsorbent surface displayed saturation for adsorbate adsorption. This model demonstrated the equilibrium distribution of analytes between the adsorbent's surface and the solution (Vermeulen et al.,1966). A finite number of adsorption sites result from a homogeneous quantity of adsorption energy, which has no relationship with coverage degree. The Langmuir adsorption model is given by the following equation:

$$Qe = \frac{QoK_{\mathrm{L}}Ce}{1 + K_{\mathrm{L}}Ce}$$

Where Qe showed the amount of adsorbate per gram adsorbed by the adsorbent at the stage of equilibrium (mg/g), Qo is the maximum monolayer adsorption capacity of the adsorbent for the adsorbate, K_{L} isotherm constant (L/mg) and Ce is the final equilibrium concentration of the analyte that remained after the adsorption. To compute the value of adsorption capacity and the isotherm constant, the plot was linear fitted concerning the equation given below:

$$\frac{1}{Q\mathrm{e}} = \frac{1}{Qo} + \frac{1}{QoK_{L}Ce}$$

Where, the plot of 1/ Q_e and 1/ C_e yields a straight line, with the slope representing K_L and the intercept indicating Q_o. R_L is computed to determine if the sorption process is favorable or unfavorable. When the R_L value exceeds one, the sorption process is unfavorable, but it is favorable when the value is less than 1. In the case of Arsenic, Adsorption studies in the Langmuir plot showed the maximum adsorption capacity of 21.37 mg/g, indicating good linearity as shown in Figure 10 with the K_L (adsorption equilibrium parameter) value of 0.9649 as shown in Table 1. The result revealed that the value of R_L is 0.0607, which is concluded to be a favorable condition for the adsorption of Arsenic on the surface of the material. Instead, the Langmuir plot for Nitrate adsorption indicates low linearity with an R^2 value of 0.82. It concluded that the adsorption was not based on the monolayer adsorption phenomenon because of a limited number of sites for the Nitrate interaction.

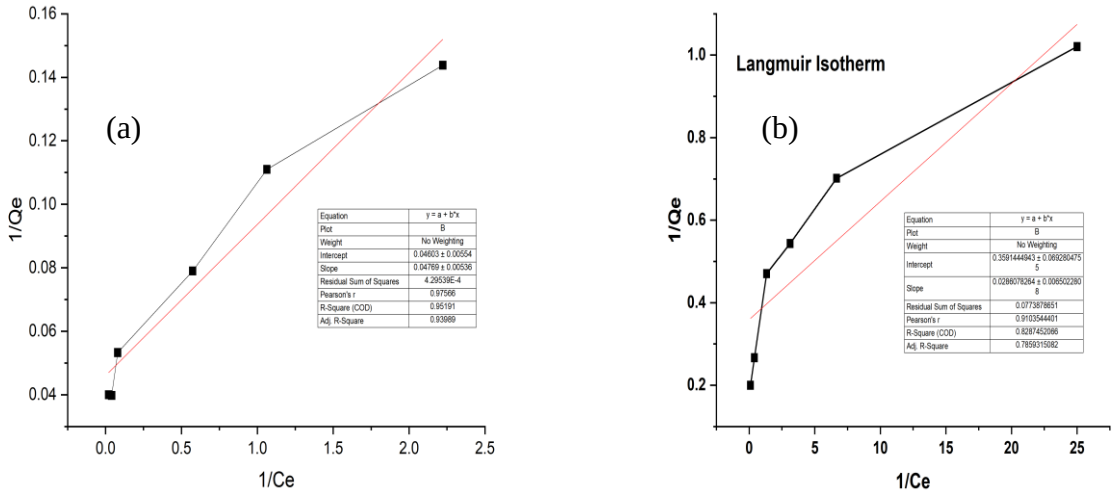

Figure 10 Langmuir adsorption isotherm plot of the Magnetic biochar-chitosan composite under optimized conditions for the removal of (a) Arsenic (b) Nitrate

5.3.2. Freundlich isotherm model

The Freundlich equation was proposed to examine the physiochemical parameters of the heterogeneous surface of the adsorbate, which is shown below.

$$Q_e = K_f C_e^{1/n}$$

Where Qe showed the amount of adsorbate per gram adsorbed by the adsorbent at the stage of equilibrium (mg/g), K_f As Freundlich isotherm constant (mg/g), the n showed the adsorption intensity and the adsorbate heterogeneity parameter.

The plot was linear and fitted between Log Qe and Log Ce, as shown by the linear equation, to quantify the strength of adsorption or heterogeneity and maximum adsorption capacity.

$$\log Qe = \log K_f + \frac{1}{n} \log C_e$$

In this equation, the intercept of the graph is used to determine the K_f value, while the slope of the Freundlich plot between Log Qe and logCe is used to calculate 1/n values that show the intensity of

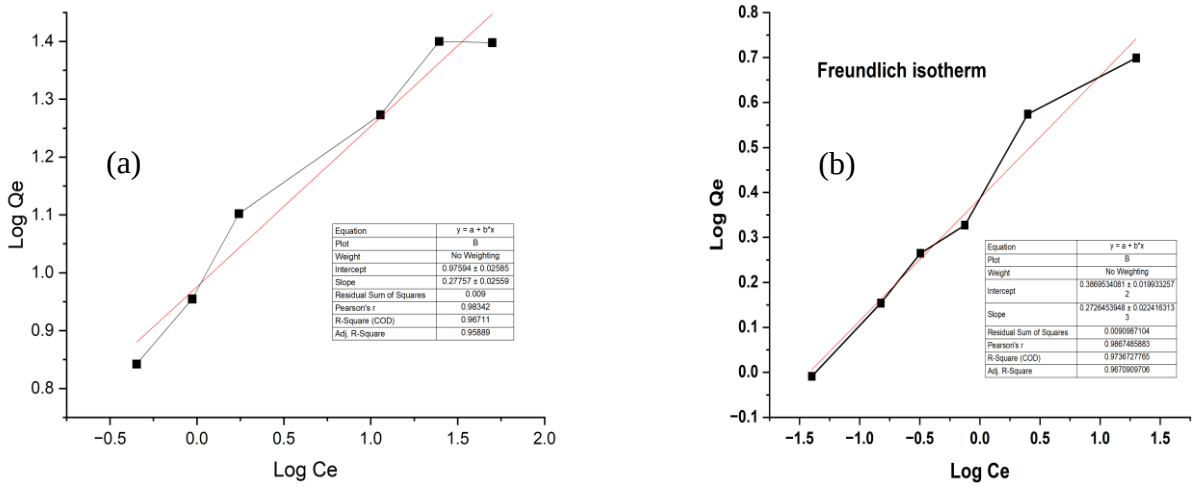

Figure 11 Freundlich adsorption isotherm plot of the Magnetic biochar-chitosan composite under optimized condtions for the removal of (a) Arsenic (b) Nitrate

adsorption. Adsorption intensity (1/n) less than 1 indicates normal adsorption, whereas values over 1 indicate cooperative adsorption.

The experimental data revealed that the Freundlich plot for Arsenic showed good linearity with an R^2 value of 0.96 and showed the surface having small heterogeneous sites for the adsorption of Arsenic on the surface of the material as shown in figure 11 (a). The values of K_f and n are parameter characteristics of either the Arsenic or Nitrate and the sorbate system. The calculated value of K_f 9.46 and 1/ n (adsorption intensity) is 0.277, showing the normal adsorption between the Arsenic and the adsorbent. The Freundlich plot for the Nitrate adsorption concluded a good linearity with an R^2 value of 0.98, indicating the Nitrate adsorption based on surface heterogeneity as shown in Table 2. The data concluded the maximum adsorption capacity for the Nitrate is 2.43 mg/g, and the small value of 1/n, i.e. 0.272, concluded the more significant heterogeneity favorable for the normal Nitrate adsorption as shown in Figure 11 (b).

5.3.3. Temkin Isotherm model

But in the case of Tamkin isotherm, the equilibrium data calculated from a linear plot against the Arsenic sorption showed an R^2 value (0.9773) as in figure 12 (a) and for nitrate it showed 0.9358 as shown in

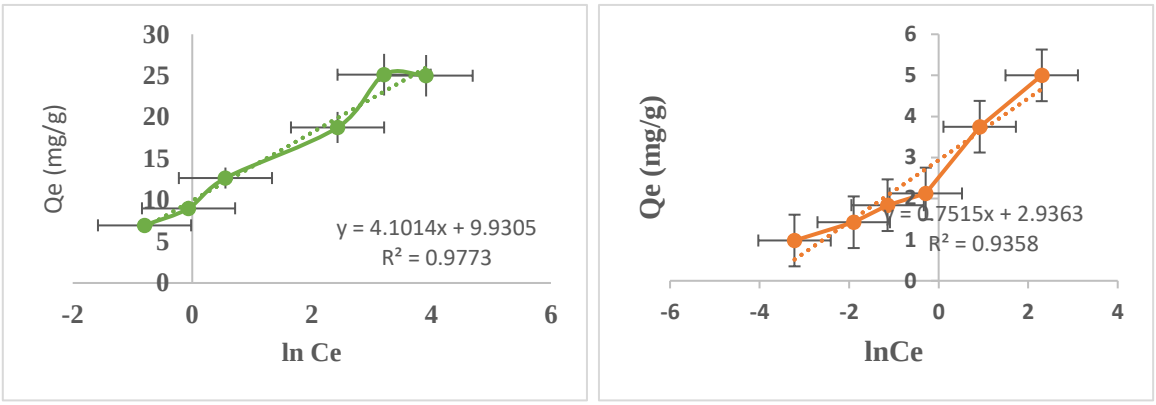

Figure 12. Temkin adsorption isotherm plot of the Magnetic biochar-chitosan composite under optimized condtions for the removal of (a) Arsenic (b) Nitrate

figure 12 (b), which suggested the adsorption was based on physisorption followed by chemisorption. As in case the adsorption study revealed the optimization condition for the removal of arsenic as pH of 10, temperature (25 °C) within 60 minutes of contact time for the 97 % of removal followed by the isotherm study which concluded that the removal of arsenic follow the Langmuir isotherm model with maximum adsorption capacity of 21.37 mg/g as shown in table 1.

Table 1. It showed the results of kinetic parameters optimization and maximum adsorbent capacity for the removal of Arsenic by waste derived composite

Sr.No.	parameters	Optimized result
1	pH	10
2	Temperature	25°C
3	Contact time	60 min
4	Adsorbent Dose	1.5 g/l
5	Removal Efficiency	97%
6	Maximum Adsorbent capacity	21.37 mg/g,
7	Isotherm model	Langmuir isotherm model (R^2 = 0.976)

But in case of nitrate removal the study revealed the optimization condition for the removal of nitrate by using the magnetic biochar and chitosan composite as pH of 7.0, temperature (25 °C) within 80 minutes of contact time for the maximum 90 % of removal followed by the isotherm study which concluded that the removal of nitrate followed the Freundlich isotherm model with maximum adsorption capacity of 2.43 mg/g as shown in table 2.

Table 2. It showed the results of kinetic parameters optimization and maximum adsorbent capacity for the removal of Nitrate by waste derived composite

Sr.No.	parameters	Optimized result
1	pH	7.0
2	Temperature	25°C
3	Contact time	80 min
4	Adsorbent Dose	2.0 g/l
5	Removal Efficiency	90 %
6	Maximum Adsorbent capacity	2.43 mg/g
7	Isotherm model	Freundlich isotherm model (R^2 = 0.98)

5.4. Application of a Rapikit for the removal of Arsenic and Nitrate.

The Rapikit is based on the principle of "Dip and treat" within minutes of contact time, where the prepared waste-derived magnetic biochar-chitosan composites adsorb both the contaminants from water. The experiment involved immersing the empty sachet and the fabricated Rapikit in a spiked solution (100 ml) having neutral pH containing Arsenic and Nitrate, specifically at concentrations of 10 ppb for Arsenic and 10 ppm for Nitrate as shown in Figure 13. The study revealed that the empty sachet showed a negligible removal efficiency for the target analytes i.e. Arsenic (1.76%) and Nitrate (0.97%), which indicated weak adsorption by the empty sachet. However, the Rapikit filled with waste-derived magnetic biochar–chitosan composite demonstrated about 90% removal of Arsenic and 50% removal of Nitrate within 10 minutes of contact time. When the time of contact was prolonged to 30 minutes it showed removal of Arsenic (97.67%) and 90% removal of Nitrate. The result showed that the synergistic presence of the both contaminants or the combined interactive forces within the mixed sachet configuration accelerates the

initial adsorption kinetics, allowing the Rapikit to hit near- equilibrium removal rate in just 30 minutes, even before the complete individual saturation is achieved.

Figure 13 depicts (a) The Empty sachet kit Dipped into Spiked solution **(**b) Rapikit filled with the waste wood derived magnetic biochar –chitosan composite dipped into spiked solution

5.5. Reusability study

To improve the cost-effectiveness of the proposed decontamination procedure, the pollutant-loaded Magnetic biochar-chitosan composite-based Rapikit was regenerated for reuse. To increase profitability, the active agent should be able to renew through desorption using the Alkaline solution (0.1 M NaOH Solution) for arsenic and 0.1 M NaCl solution for displaced adsorbed Anions through the anion exchange without compromising material integrity.

Keeping the above points in mind, the recyclability of the Rapikit was tested with several desorption reagents, including acid, basic, and phosphate media, at varying concentrations and volumes. The reusability study was checked for five removal cycles. It showed the percentages of removal efficiency calculated as 90%, 90 %, 88%, 85%, and 80%. There was no decrease in removal effectiveness after as many as five cycles, and adsorbent loss during adsorption and desorption was minimal, as shown in Figure 14.

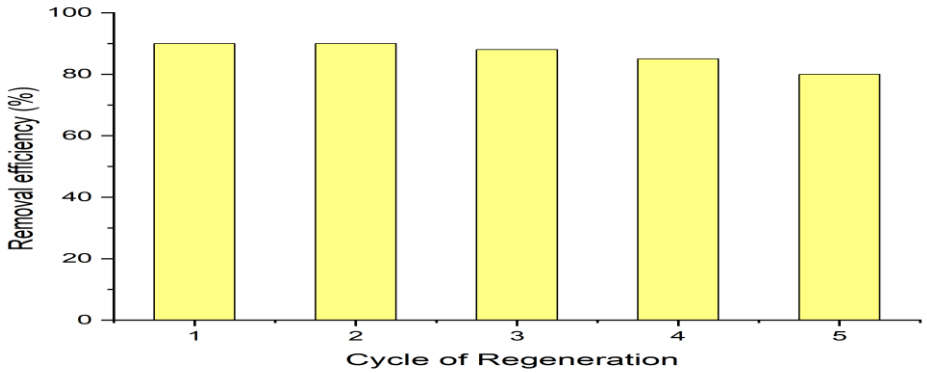

Figure 14 Graphical representation of the reusability study of the magnetic biochar-chitosan composite based Rapikit w.r.t. removal efficiency against 5 cycle.

As shown in Table 3, the developed composite exhibited a significantly higher removal efficiency (97% for arsenic and 90% for nitrate) as compared with the most reported adsorbents, which generally showed less removal efficiency for nitrate as well as arsenic and also only removed one of the contaminants. But in case of our developed composite it showed superior removal performance and dual removal which may be attributed to the synergistic effect of magnetic biochar and chitosan, providing abundant active sites and enhanced surface interaction with the analytes.

Table 3. It showed the Comparison of various adsorbents used for the removal of Arsenic and Nitrate

Sr.No.	Contaminants	Adsorbent	Removal efficiency (%)	pH	References
1	As(III)	Magnetic Biochar	94.9	9.0	[48]
2	As(III)	Magnetic Biochar Fe_2MnC (Waste wood)	81	7.0	[49]
3	As(III)	Magnetic Biochar Fe_1Mn_4C	80.8	3.0	[49]
4	As(III)	Magnetic Chitosan composite	96.73	4.0	[50]
5	NO_3^-	Garden waste derived biochar	62.11	2.0	[51]
6	NO_3^-	Hydrogel rice husk biochar composite	34.3	3.0	[52]
7	NO_3^-	Chitosan Zeolite composites	40.28	-	[53]
8	NO_3^-	Chitosan	66.9	-	[54]
		Bentonites	49.5		
9	**As(III) + NO_3^-**	**Waste derived magnetic biochar-chitosan composite (Rapi-Kit)**	**97.67 % (As(III)) / 90% (NO_3^-)**	**6.9**	**Our Work**

Conclusion

The present study demonstrates the high effectiveness of the Rapikit filled of Waste derived magnetic biochar-chitosan composite for the removal of Nitrate as well as Arsenic from the water. The fabricated Rapikit showed 97.67 % removal of arsenic and 90 % of Nitrate within 30 minutes of contact time for 10 ppb arsenic and 10 ppm of Nitrate spiked solution. The characterization techniques approve the modification by analyzing the surface topography as well as the functional group analysis of the composite material. The waste derived composite in the batch study, showed 97 % removal efficiency for the Arsenic under optimized conditions such as pH 10 and 60 minutes of contact time with a 1.5g/l dose of adsorbent. In the case of Nitrate effectiveness, around 90 % removal efficiency was found under optimized conditions such as pH 7, a contact time of 80 minutes with 2.0g/l dose of adsorbent. The equilibrium data plotted against the isotherm models revealed that the adsorption of Arsenic well fitted with the Langmuir isotherm model, showing the maximum adsorption capacity of 21.37 mg/g and R_L (0.0607), which concluded the favorable condition for the adsorption of Arsenic. However, in the case of Nitrate, the equilibrium data was well fitted with the Freundlich isotherm, having good linearity with an R^2 value of 0.98, indicating the Nitrate adsorption based on surface heterogeneity. The data concluded the maximum adsorption capacity for the Nitrate is 2.43 mg/g. Batch studies include drawbacks, such as a filtration procedure and drying of the material. Therefore the Rapikit offer a portable sustained user friendly solution for the dual removal functionality for the arsenic and nitrate. The result is the enhanced efficiency for removal and paving the way for more sustainable, cost-effective, and scalable solutions in future water decontamination technologies.

Author's declaration. All authors have read, understood, and compiled, as applicable, the statement on the ethical responsibilities of authors. The paper has not been published elsewhere. They acknowledge the work's originality and say that it does not infringe on any copyright or property rights nor utilize any ideas, techniques, quotes, or other information from other sources without permission.

Conflict of interest: The authors have no competing interests to declare relevant to this research article's content.

Declaration of funding: This research did not receive funds, grants, or other support from funding agencies or the organization.

Data availability: The data supporting this study's conclusion are not publicly available owing to sensitivity concerns but are available from the corresponding author upon reasonable request.

Ethical approval and consent to participate: Not Applicable

Consent of Publication: All authors of this manuscript have consented to publication.

REFERENCES:

[1] S. Sharma and A. Bhattacharya, "Drinking water contamination and treatment techniques," Appl. Water Sci., vol. 7, no. 3, pp. 1043–1067, 2017, doi: 10.1007/s13201-016-0455-7.

[2] P. Zhang et al., "Water Quality Degradation Due to Heavy Metal Contamination: Health Impacts and Eco-Friendly Approaches for Heavy Metal Remediation," Toxics, vol. 11, no. 10, 2023, doi: 10.3390/toxics11100828.

[3] V. Kumar et al., "Removal of Inorganic Pollutants from Wastewater: Innovative Technologies and Toxicity Assessment," Sustain., vol. 15, no. 23, 2023, doi: 10.3390/su152316376.

[4] M. Farhan Hanafi and N. Sapawe, "A review on the water problem associate with organic pollutants derived from phenol, methyl orange, and remazol brilliant blue dyes," Mater. Today Proc., vol. 31, no. 2020, pp. A141–A150, 2020, doi: 10.1016/j.matpr.2021.01.258.
[5] rehan rashid Jan habib, ullah nehar, "Impact of Industrial Effluents Discharge on Ground Water Quality," no. February, 2021.
[6] K. S. Mohammed Abdul, S. S. Jayasinghe, E. P. S. Chandana, C. Jayasumana, and P. M. C. S. De Silva, "Arsenic and human health effects: A review," Environ. Toxicol. Pharmacol., vol. 40, no. 3, pp. 828–846, 2015, doi: 10.1016/j.etap.2015.09.016.
[7] L. Fewtrell, "Drinking-water nitrate, methemoglobinemia, and global burden of disease: A discussion," Environ. Health Perspect., vol. 112, no. 14, pp. 1371–1374, 2004, doi: 10.1289/ehp.7216.
[8] M. H. Ward et al., "Drinking water nitrate and human health: An updated review," Int. J. Environ. Res. Public Health, vol. 15, no. 7, pp. 1–31, 2018, doi: 10.3390/ijerph15071557.
[9] K. Fytianos and C. Christophoridis, "Nitrate, arsenic and chloride pollution of drinking water northern Greece. Elaboration by applying gis," Environ. Monit. Assess., vol. 93, no. 1–3, pp. 55–67, 2004, doi: 10.1023/B:EMAS.0000016791.73493.aa.
[10] J. Wang, X. Liu, A. H. W. Beusen, and J. J. Middelburg, "Surface-Water Nitrate Exposure to World Populations Has Expanded and Intensified during 1970-2010," Environ. Sci. Technol., vol. 57, no. 48, pp. 19395–19406, 2023, doi: 10.1021/acs.est.3c06150.
[11] WHO World Health Organization, "Preventing Disease through Healthy Environment. Exposure to Arsenic: A Major Public Health Concern," Prev. Dis. through Heal. Environ., pp. 1–5, 2019, [Online]. Available: http://www.who.int/ipcs/features/arsenic.pdf?ua=1
[12] Bijay-Singh and E. Craswell, "Fertilizers and nitrate pollution of surface and ground water: an increasingly pervasive global problem," SN Appl. Sci., vol. 3, no. 4, pp. 1–24, 2021, doi: 10.1007/s42452-021-04521-8.
[13] J. Lakshmi, G. Sozhan, and S. Vasudevan, "Recovery of hydrogen and removal of nitrate from water by electrocoagulation process," Environ. Sci. Pollut. Res., vol. 20, no. 4, pp. 2184–2192, 2013, doi: 10.1007/s11356-012-1028-4.
[14] E. Lacasa, P. Cañizares, C. Sáez, F. J. Fernández, and M. A. Rodrigo, "Removal of nitrates from groundwater by electrocoagulation," Chem. Eng. J., vol. 171, no. 3, pp. 1012–1017, 2011, doi: 10.1016/j.cej.2011.04.053.
[15] G. A. C. Madlangbayan, K. G. N. Quiton, and M. C. Lu, "Removal of Lead and Nitrate from Simulated Lead- and Nitrate-Containing Wastewater via Hydroxide Precipitation," Processes, vol. 12, no. 8, pp. 1–13, 2024, doi: 10.3390/pr12081662.
[16] S. Samatya, N. Kabay, Ü. Yüksel, M. Arda, and M. Yüksel, "Removal of nitrate from aqueous solution by nitrate selective ion exchange resins," React. Funct. Polym., vol. 66, no. 11, pp. 1206–1214, 2006, doi: 10.1016/j.reactfunctpolym.2006.03.009.
[17] R. B. Gauntlett, "Nitrate removal from water by ion exchange," Water Treatm.Exam., vol. 24, no. 3 pt 3, pp. 172–193, 1975, doi: 10.17508/cjfst.2017.9.2.15.
[18] A. Abejón, A. Garea, and A. Irabien, "Arsenic removal from drinking water by reverse osmosis: Minimization of costs and energy consumption," Sep. Purif. Technol., vol. 144, pp. 46–53, 2015, doi: 10.1016/j.seppur.2015.02.017.

[19] A. Matei and G. Racoviteanu, "Review of the technologies for nitrates removal from water intended for human consumption," IOP Conf. Ser. Earth Environ. Sci., vol. 664, no. 1, 2021, doi: 10.1088/1755-1315/664/1/012024.
[20] J. J. Schoeman and A. Steyn, "Nitrate removal with reverse osmosis in a rural area in South Africa," Desalination, vol. 155, no. 1, pp. 15–26, 2003, doi: 10.1016/S0011-9164(03)00235-2.
[21] R. Epsztein, O. Nir, O. Lahav, and M. Green, "Selective nitrate removal from groundwater using a hybrid nanofiltration-reverse osmosis filtration scheme," Chem. Eng. J., vol. 279, pp. 372–378, 2015, doi: 10.1016/j.cej.2015.05.010.
[22] M. Aliaskari and A. I. Schäfer, "Nitrate, arsenic and fluoride removal by electrodialysis from brackish groundwater," Water Res., vol. 190, 2021, doi: 10.1016/j.watres.2020.116683.
[23] I. Ali, T. A. Khan, and M. Asim, "Removal of arsenic from water by electrocoagulation and electrodialysis techniques," Sep. Purif. Rev., vol. 40, no. 1, pp. 25–42, 2011, doi: 10.1080/15422119.2011.542738.
[24] J. Bi, C. Peng, H. Xu, and A. S. Ahmed, "Removal of nitrate from groundwater using the technology of electrodialysis and electrodeionization," Desalin. Water Treat., vol. 34, no. 1–3, pp. 394–401, 2011, doi: 10.5004/dwt.2011.2891.
[25] N. Kumar, A. Kardam, V. K. Jain, and S. Nagpal, "A rapid, reusable polyaniline-impregnated nanocellulose composite-based system for enhanced removal of chromium and cleaning of waste water," Sep. Sci. Technol., vol. 55, no. 8, pp. 1436–1448, 2020, doi: 10.1080/01496395.2019.1600552.
[26] R. Rahul, R. Kumar, and S. Nagpal, "The Removal of Fluoride from the Water Using Epipremnum aureum (Money Plant)," Water Conserv. Sci. Eng., vol. 8, no. 1, pp. 1–8, 2023, doi: 10.1007/s41101-023-00221-z.
[27] R. Khatkar and S. Nagpal, "Defluorination Techniques: Past, Present and Future Prospective," Korean J. Chem. Eng., vol. 41, no. 3, pp. 553–569, 2024, doi: 10.1007/s11814-024-00106-4.
[28] H. Zhu, Y. Jia, X. Wu, and H. Wang, "Removal of arsenic from water by supported nano zero-valent iron on activated carbon," J. Hazard. Mater., vol. 172, no. 2–3, pp. 1591–1596, 2009, doi: 10.1016/j.jhazmat.2009.08.031.
[29] M. Mazarji, B. Aminzadeh, M. Baghdadi, and A. Bhatnagar, "Removal of nitrate from aqueous solution using modified granular activated carbon," J. Mol. Liq., vol. 233, pp. 139–148, 2017, doi: 10.1016/j.molliq.2017.03.004.
[30] C. V. Lazaratou, D. V. Vayenas, and D. Papoulis, "The role of clays, clay minerals and clay-based materials for nitrate removal from water systems: A review," Appl. Clay Sci., vol. 185, no. June, p. 105377, 2020, doi: 10.1016/j.clay.2019.105377.
[31] P. K. Tandon, R. C. Shukla, and S. B. Singh, "Removal of arsenic(III) from water with clay-supported zerovalent iron nanoparticles synthesized with the help of tea liquor," Ind. Eng. Chem. Res., vol. 52, no. 30, pp. 10052–10058, 2013, doi: 10.1021/ie400702k.
[32] M. Bilici Baskan and A. Pala, "Removal of arsenic from drinking water using modified natural zeolite," Desalination, vol. 281, no. 1, pp. 396–403, 2011, doi: 10.1016/j.desal.2011.08.015.
[33] J. Schick, P. Caullet, J. L. Paillaud, J. Patarin, and C. Mangold-Callarec, "Batch-wise nitrate removal from water on a surfactant-modified zeolite," Microporous Mesoporous Mater., vol. 132, no. 3, pp. 395–400, 2010, doi: 10.1016/j.micromeso.2010.03.018.

[34] A. Sowmya and S. Meenakshi, "Effective removal of nitrate and phosphate anions from aqueous solutions using functionalised chitosan beads," Desalin. Water Treat., vol. 52, no. 13–15, pp. 2583–2593, 2014, doi: 10.1080/19443994.2013.798842.
[35] A. Ayub et al., Arsenic in drinking water: overview of removal strategies and role of chitosan biosorbent for its remediation, vol. 29, no. 43. Springer Berlin Heidelberg, 2022. doi: 10.1007/s11356-022-21988-z.
[36] M. Habuda-Stanić and M. Nujić, "Arsenic removal by nanoparticles: a review," Environ. Sci. Pollut. Res., vol. 22, no. 11, pp. 8094–8123, 2015, doi: 10.1007/s11356-015-4307-z.
[37] S. Tyagi, D. Rawtani, N. Khatri, and M. Tharmavaram, "Journal of Water Process Engineering Strategies for Nitrate removal from aqueous environment using Nanotechnology : A Review," J. Water Process Eng., vol. 21, no. December 2017, pp. 84–95, 2018, doi: 10.1016/j.jwpe.2017.12.005.
[38] L. Divband Hafshejani, A. Hooshmand, A. A. Naseri, A. S. Mohammadi, F. Abbasi, and A. Bhatnagar, "Removal of nitrate from aqueous solution by modified sugarcane bagasse biochar," Ecol. Eng., vol. 95, pp. 101–111, 2016, doi: 10.1016/j.ecoleng.2016.06.035.
[39] J. Alchouron et al., Household arsenic contaminated water treatment employing iron oxide/bamboo biochar composite: An approach to technology transfer, vol. 587. Elsevier Inc., 2021. doi: 10.1016/j.jcis.2020.11.036.
[40] S. Jodeh, I. Ibsharat, B. Khalaf, O. Hamed, D. Jodeh, and D. Omar, "The Use of Magnetic Multiwalled Carbon Nanotubes Functionalized with Chitosan for Nitrate Removal from Wastewater," Chem. Africa, vol. 2, no. 3, pp. 321–333, 2019, doi: 10.1007/s42250-019-00056-z.
[41] N. Sankararamakrishnan, A. Gupta, and S. R. Vidyarthi, "Enhanced arsenic removal at neutral pH using functionalized multiwalled carbon nanotubes," J. Environ. Chem. Eng., vol. 2, no. 2, pp. 802–810, 2014, doi: 10.1016/j.jece.2014.02.010.
[42] L. Liang, F. Xi, W. Tan, X. Meng, B. Hu, and X. Wang, "Review of organic and inorganic pollutants removal by biochar and biochar-based composites," Biochar, vol. 3, no. 3, pp. 255–281, 2021, doi: 10.1007/s42773-021-00101-6.
[43] A. B. D. Nandiyanto, R. Ragadhita, and M. Fiandini, "Interpretation of Fourier Transform Infrared Spectra (FTIR): A Practical Approach in the Polymer/Plastic Thermal Decomposition," Indones. J. Sci. Technol., vol. 8, no. 1, pp. 113–126, 2023, doi: 10.17509/ijost.v8i1.53297.
[44] A. Azari et al., "Magnetic adsorption separation process: an alternative method of mercury extracting from aqueous solution using modified chitosan coated Fe3O4 nanocomposites," J. Chem. Technol. Biotechnol., vol. 92, no. 1, pp. 188–200, 2017, doi: 10.1002/jctb.4990.
[45] B. Li et al., "Synthesis, characterization, and antibacterial activity of cross-linked chitosan-glutaraldehyde," Mar. Drugs, vol. 11, no. 5, pp. 1534–1552, 2013, doi: 10.3390/md11051534.
[46] G. S. dos Reis et al., "Preparation of highly porous nitrogen-doped biochar derived from birch tree wastes with superior dye removal performance," Colloids Surfaces A Physicochem. Eng. Asp., vol. 669, no. June, p. 131493, 2023, doi: 10.1016/j.colsurfa.2023.131493.
[47] A. L. Srivastav, T. D. Pham, S. C. Izah, N. Singh, and P. K. Singh, "Biochar Adsorbents for Arsenic Removal from Water Environment: A Review," Bull. Environ. Contam. Toxicol., vol. 108, no. 4, pp. 616–628, 2022, doi: 10.1007/s00128-021-03374-6.

[48] H. Kim, E. Myung, N. Choi, and K. Cho, "Removal of arsenic from aqueous solution using magnetic biochar derived from Spirulina platensis," J. Hazard. Mater. Adv., vol. 16, no. September, p. 100490, 2024, doi: 10.1016/j.hazadv.2024.100490.
[49] C. K. Chen, J. J. Chen, N. T. Nguyen, T. T. Le, N. C. Nguyen, and C. T. Chang, "Specifically designed magnetic biochar from waste wood for arsenic removal," Sustain. Environ. Res., vol. 31, no. 1, 2021, doi: 10.1186/s42834-021-00100-z.
[50] L. M. Tri, P. Thi Mai Huong, and N. Thi Huong, "Magnetic Chitosan Nanocomposites Derived from Industrial Solid Waste: A Promising Approach for Arsenic(III) Remediation," ACS Omega, vol. 10, no. 4, pp. 3351–3360, 2025, doi: 10.1021/acsomega.4c05955.
[51] J. Yao, Z. Wang, M. Liu, B. Bai, and C. Zhang, "Nitrate-Nitrogen Adsorption Characteristics and Mechanisms of Various Garden Waste Biochars," Materials (Basel)., vol. 16, no. 16, 2023, doi: 10.3390/ma16165726.
[52] M. J. Z.-M. Mahsa Sadeghi Afjeh Gholam Bagheri Marandi, "Nitrate removal from aqueous solutions by adsorption onto hydrogel-rice husk biochar composite," Water Environ. Res., vol. 92, pp. 934–937, 2020.
[53] Y. Gao, Y. Ru, L. Zhou, X. Wang, and J. Wang, "Preparation and Characterization of Chitosan-Zeolite Molecular Sieve Composite for Ammonia and Nitrate Removal," Adv. Compos. Lett., vol. 27, no. 5, 2018, doi: 10.1177/096369351802700502.
[54] B. Nagaraja, K. R. Reddy, and A. M. Palomino, "Nitrate Removal from Stormwater Using Chitosan and Bentonite," Geotech. Front., pp. 89–98, 2025, doi: 10.1061/9780784486009.010.